Chapter Seven
Reaustenitisation in Bainitic Steels

7.1 Introduction

Work on reaustenitisation in high-strength steel weld deposits has been reported in Chapter 4 and 5. In this chapter, reaustenitisation in bainitic steels is investigated further. Bainitic ferrite possesses high strength and high toughness properties especially in some silicon containing alloy steels [176,177]. The microstructures have been exploited to improve mechanical properties compared with those of conventional tempered martensite based microstructures. In order to develop these bainitic steels in the construction of submarines, off-shore plateforms and many other applications, their weldability is crucial.

The specific aim of the present work is to elucidate the effect of the carbon content of residual austenite on reaustenitisation in bainitic steels which contain high concentrations of silicon. The high silicon concentration allows transformation to first bainitic ferrite and residual austenite (i.e., no carbides). If this microstructure is, without cooling from the isothermal transformation temperature, rapidly reheaded then the reaustenitisation process requires no nucleation of austenite, permitting a controlled study of the growth of austenite. On the other hand, the mixture of bainite and austenite can be tempered to decompose the austenite into ferrite plus carbide; reaustenitisation of the resultant microstructure ferrite plus carbide would then require the nucleation of austenite, permitting a study of nucleation effects. Both isothermal and continuous heating experiments have been carried out.

7.2 Experimental Procedure

The experimental details are essentially the same as in Section 4.2 and 5.3, and are not restated here. The steels used were prepared from high purity base materials as 20 kg vacuum induction melts and were hot worked to 8mm diameter rod. The ingots were sealed in quartz capsules (under a partial pressure of argon) and homogenised for three days at 1250°C, before hot reduction to 3.2mm diameter rods. The chemical composition of the alloy studied is Fe-0.43C-3.00Mn-2.02Si, wt.%.

7.3 Results and Discussion

7.3.1 The Nature of Bainite (α_b)

Figure VII.1a shows the isothermal transformation curves of bainite for the alloy austenitised at 950°C for 10 minutes followed by isothermal transformation at 350, 380

and 410°C, respectively. The maximum extent of transformation to upper bainite increases as the transformation temperature decreases. In steels where the bainite transformation can develop without interference from other reactions, this is known to exhibit an "incomplete reaction phenomenon" [25,89,100]; in this, the transformation stops prematurely, well before the carbon concentration of the residual austenite (X_γ) reaches its equilibrium or paraequilibrium concentration. The transformation stops when X_γ reaches approximately a concentration (X_{T_0}) given by T_0 curve on the phase diagram. The T_0 curve on a plot of temperature versus carbon concentration represents the locus of all points where ferrite and austenite of the same composition have equal free energy. To take account of invariant-plane strain shape change accompanying the formation of bainite, a T'_0 curve is defined in which the free energy of ferrite is increased by 400 J/mol [100]. In the present work, it is found that for the alloy studies the bainite transformation terminates when the X_γ reaches T_0 curve (Figure VII.1b). This can be expected due to plastic relaxation and interactions between sheaves of bainite [180].

It was noted that the alloy required about 30 minutes to achieve maximum transformation at 350°C. An upper bainite microstructure (Figure VII.2) was obtained following isothermal transformation at 350°C for 120 minutes. The microstructure was a mixture of 55% bainitic ferrite and 45% residual austenite (some of the residual austenite transformed to martensite during cooling), as determined by the techniques discussed in Section 3.2. Austenite was found to occur in two forms: blocky and film morphologies (Figure VII.2). The former originates from the geometrical partitioning of the prior austenite grain by sheaves of bainite whereas the latter is confined between bainitic ferrite subunits (Figure VII.3). Although there are two kind morphologies of austenite, the carbon content of all forms of austenite may be expected to be the same.

7.3.2 Reaustenitisation by Continuous Heating

If after isothermal transformation to bainite at 350°C for only 10 minutes, the specimen is continuously heated, the residual austenite is found to decompose during heating, before the onset of reaustenitisation. This was found to be particularly the case with low heating rates as shown in Figure VII.4. Figures VII.4a and b present the relative length change versus temperature curves for continuous heating at heating rates of 0.06 and 0.15°C/s, respectively, after isothermal transformation at 350°C for 10 minutes. A pearlite-like microstructure formed (Figure VII.5a) from the large regions of blocky residual austenite when the temperature reached about 600°C at a heating rate of 0.06°C/s. This was expected because the starting microstructure contained a high volume fraction of relatively low carbon untransformed austenite, since the specimen had only been transformed to a low volume fraction of bainitic ferrite. It was also found that the film

159

austenite had decomposed into bands of discretely nucleated carbides in the same condition (Figure VII.5b).

Figures VII.6a and b present the continuous heating curves for samples transformed isothermally to bainite at 350°C for 120 minutes, followed immediately by continuous heating at 0.06 and 0.15°C/s, respectively. The results also demonstrate that the relative length change versus temperature curves deviate from linearity during heating before the process of reaustenitisation begins in both the experiments. The deviations indicate decomposition of austenite during heating. Figures VII.7, 8 and 9 show the electron micrographs corresponding to Figure VII.6a (heating rate = 0.06°C/s) from specimens which were quenched after temperature reaching 600, 700 and 730°C, respectively. Such slow heating also leads to the diffusional decomposition of high carbon residual austenite into tiny particles of carbides (Figure VII.7) located between bainitic ferrite plates. Micrograph (Figure VII.8) shows that the carbide particle coalesce along the bainitic ferrite boundaries when a temperature as high as 700°C is reached. The austenite forms from the larger elongated carbide particles (Figure VII.9) as the temperature rises beyond 720°C.

In order to elucidate the effect of carbon content of residual austenite on reaustenitisation, specimens austenitised at 950°C for 10 minutes were isothermally transformed to bainite for 120 minutes (i.e., longer than needed to complete the bainitic reaction). Figure VII.10 shows the reaustenitisation start temperature versus heating rate for four different starting microstructures, which are three bainite microstructures and one tempered bainite microstructure (Figure VII.11). It is clear that the carbon content of residual austenite influences the reaustenitisation behaviour. Because of the negative slope of T_0 curve, for the higher bainitic transformation temperature the lower carbon content of residual austenite is obtained. It was expected that the bainite formed at higher temperature should be reaustenitised at a higher temperature (Figure VII.12), as predicted by the theoretical analysis mentioned in Section 4.3. As the heating rate is lower than 0.6°C/s, these three bainite structures have nearly the same reaustenitisation temperature (Figure VII.10), simply because the residual austenite first decomposes to ferrite plus carbide during heating before the onset of reaustenitisation. Figure VII.11 shows carbide particles in tempered bainite; the elongated carbide particles were formed from carbon-enriched residual austenite, and the tiny carbide particles precipitated in supersaturated bainitic ferrite plates. When the tempered bainite is heated at a fast heating rate, the reaustenitisation start temperature is higher than that of bainite structure. This is probably because the effect of austenite nucleation retards the rate of reaustenitisation.

7.3.3 Isothermal Reaustenitisation

Specimens austenitised at 950°C for 10 minutes were isothermally transformed to bainite at temperature 350°C for 2 hours and then, without cooling below 350°C, rapidly up-quenched to a higher temperature for isothermal reaustenitisation. Some of the dilatometric curves are shown in Figure VII.13. Some length changes were detected dilatometrically even at relatively low isothermal transformation temperature, but for the temperature less than 720°C, electron microscopies (Figures VII.14a and b) showed that the length changes were due to the diffusional decomposition of austenite into ferrite plus carbide, rather than due to reaustenitisation. When the isothermal transformation was at 720°C, the thickness of austenite layer increased slightly and no carbide particles could be found (Figure VII.14c). Therefore, the lowest isothermal reaustenitisation temperature is found to be 720°C. This is consistent with the theoretical analysis as shown by point a in Figure VII.12. Electron micrographs of Figures VII.14d, e and f show the austenite growth at 750, 780 and 800°C, respectively for 2 hours. The result of isothermal reaustenitisation at 820°C for 2 hours is shown in Figures VII.14g and h. It demonstrates that full reaustenitisation can not be complete in such condition. Even after isothermal reaustenitisation at 835°C for 6.5 hours, a little ferrite could still be found (Figure VII.14i). However, if the specimen was isothermally reaustenitised at 780°C for 1 week, after isothermally transformed to bainite at 350°C for 2 hours, the alloy became fully austenitic (Figure VII.15). The results are consistent with the fact that the last stages of reaustenitisation, which involve the long-range diffusion of substitutional elements, are tortuously slow, but a fully austenitic sample can be obtained at 780°C, consistent with theory (point b, Figure VII.12).

Microanalytical measurements have been carried out using energy dispersive X-ray analysis on a Philips EM400T transmission electron microscope. The technique has been mentioned in Chapter Two, and will not be restated here. The microanalytical data (Figure VII.16 and Table VII.1) cover a range of isothermal reaustenitisation temperatures. The results show that for 2 hours of transformation time, the degree of partitioning of alloying elements (as indicated by the deviation of the partition coefficient ki from unity, where ki $= Xi^{\gamma}/Xi^{\alpha}$) decreases with increasing reaustenitisation temperature. At 835°C for 2 hours, the partition coefficient for Mn is close to unity, but that for Si still significantly deviates from unity. The results are generally consistent with the hypothesis that less partitioning can be tolerated during transformation at higher driving forces (higher temperature in the present context).

7.3.4 Coalescence of Carbides

In Section 7.3.2, it was demonstrated that when a slow heating rate was used for the reaustenitisation of a mixture of bainitic ferrite plus residual austenite, the residual austenite decomposed into bands of discretely nucleated carbides (Figure VII.7), and then the carbide particles coalesced into an elongated morphology (Figures VII.8 and 9) along the original bainitic ferrite boundary before the onset of austenitisation. At higher heating rates, coalescence was not observed, the size of the carbide particles being small, and their shape being equiaxed. Due to the surface energy contribution to the bulk free energy necessary for the formation of stable austenite nuclei, the tiny carbide particles seem to be not easily transformed to austenite.

In order to study the coalescence of carbides to form elongated particles, further experiments have been done. Figure VII.17 shows the tempered bainite microstructure which was formed by isothermal transformation at 350°C for 2 hours and subsequently tempered at 600°C for 42.7 hours. Although the majority of carbide particles have coalesced into elongated forms, some small equiaxed particles remain. Figure VII.18 shows that after tempering the bainite at 680°C for 14 days, the carbide particles become plump (about 0.2μm thick and 0.5μm long) and are located at the grain boundaries of extensively recovered ferrite. However, after tempering the bainite at 600°C for 30 minutes and then annealing at 715°C for 25 minutes, the carbide particles combine and become extremely long (Figure VII.19-23) as was observed for the reaustenitisation experiments carried out at slow heating rates. These long particles have been proved to be cementite. They grow in a specific direction, and are parallel each other. The morphology is similar to that of pearlite, except that pearlite possesses three dimensionally continuous lamellar layers of cementite. Further work is needed to analyse the detailed orientation relationship between the long particles of cementite and the matrix ferrite, and in order to understand the growth mechanism.

7.4 Summary and Conclusions

The process of reaustenitisation from bainite in a silicon steel has been investigated, and the results are found to be consistent with the theory developed earlier. Reaustenitisation only begins when the carbon concentration of the residual austenite exceeds its equilibrium carbon concentration. The experimental results can also be explained by the theoretical model presented in Section 4.3. Due to the high level of alloying additions, the complete transformation to austenite at the Ae_3 temperature of the alloy takes an extremely long time. Microanalytical data show that the partition coefficient decreases as the driving force for transformation increases. The decomposition of residual

austenite during slow heating has also been studied. At slow heating rates, the residual austenite decompose into bands of discretely nucleated carbides, then the carbide particles coalesce along original bainitic ferrite boundaries, and finally transformed to austenite as the temperature rises.
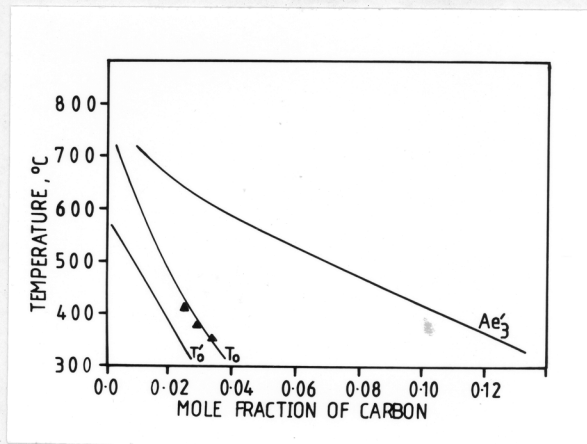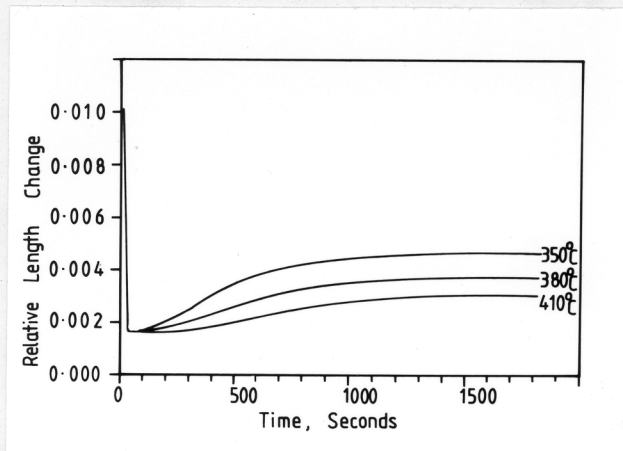
Figures VII.1 - (a) Dilatometric curves showing isothermal transformation to bainite after austenitisation at 950°C for 10 minutes. (b) Calculated phase diagram for Fe-0.43C-3.00Mn-2.02Si, and experimental data indicating that the transformation to bainite stops when X_γ reaches the T_o curve.

Figure VII.2 - Optical micrograph showing the upper bainitic ferrite and residual austenite (blocky and film morphologies) following isothermal transformation at 350°C for 120 minutes.

164

a

b

0·5µm
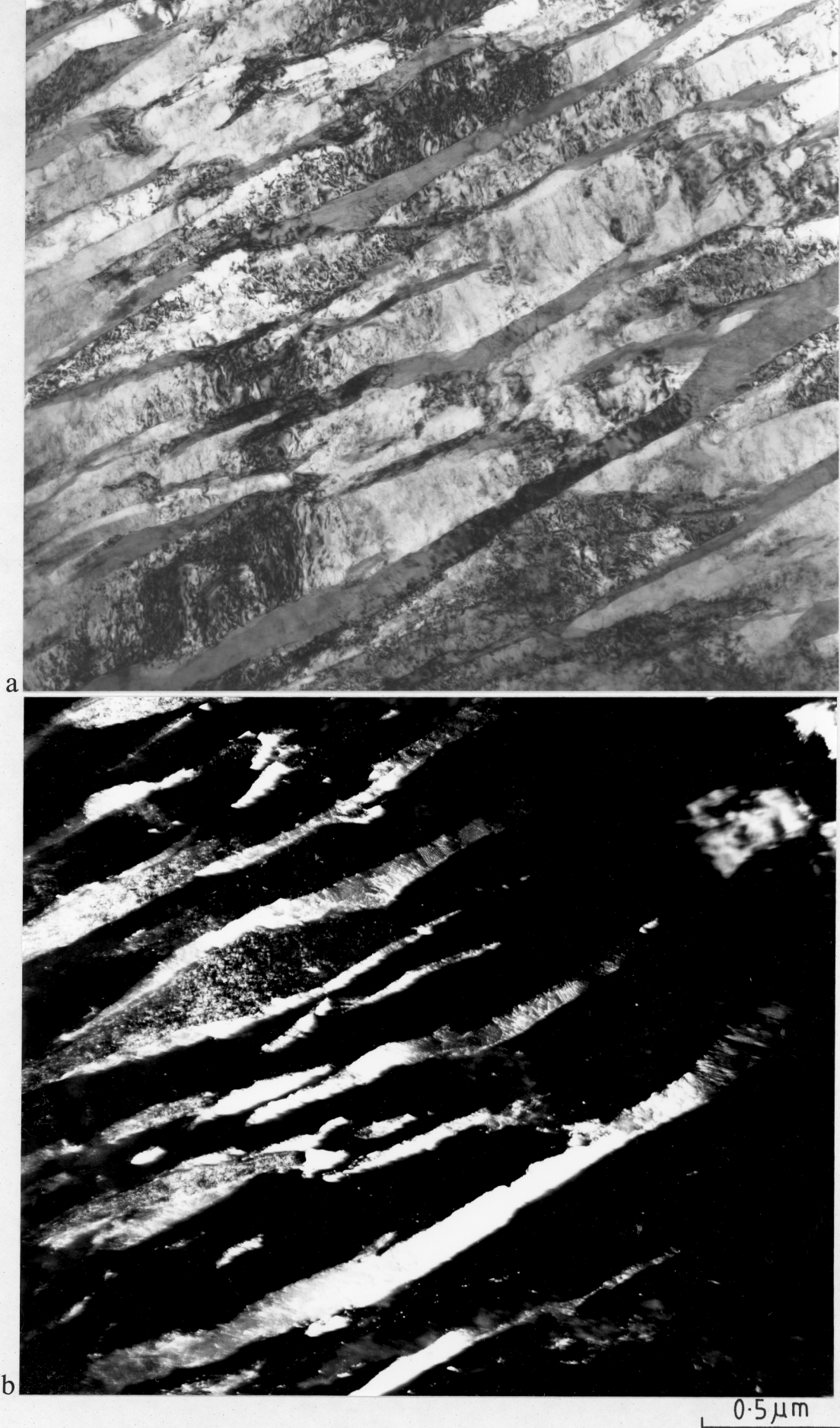
Figure VII.3 - Typical upper bainite microstructure of Fe-0.43C-3.00Mn-2.02Si alloy. (a) Bright field image of an isothermally transformed (at 350°C for 120 mins) specimen. (b) Corresponding retained austenite dark field image.

(a)

Relative Length Change

Temperature, ^{O}C

(b)

Relative Length Change
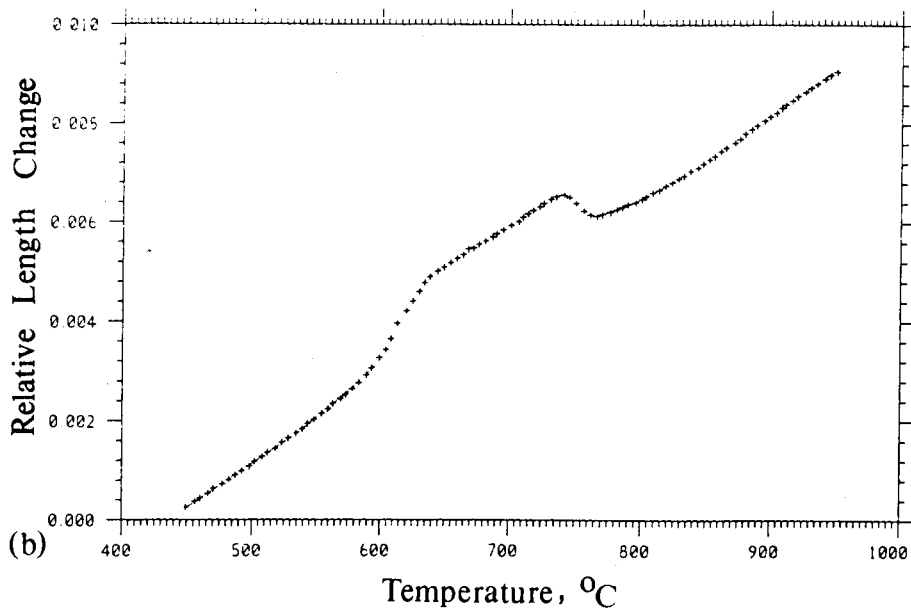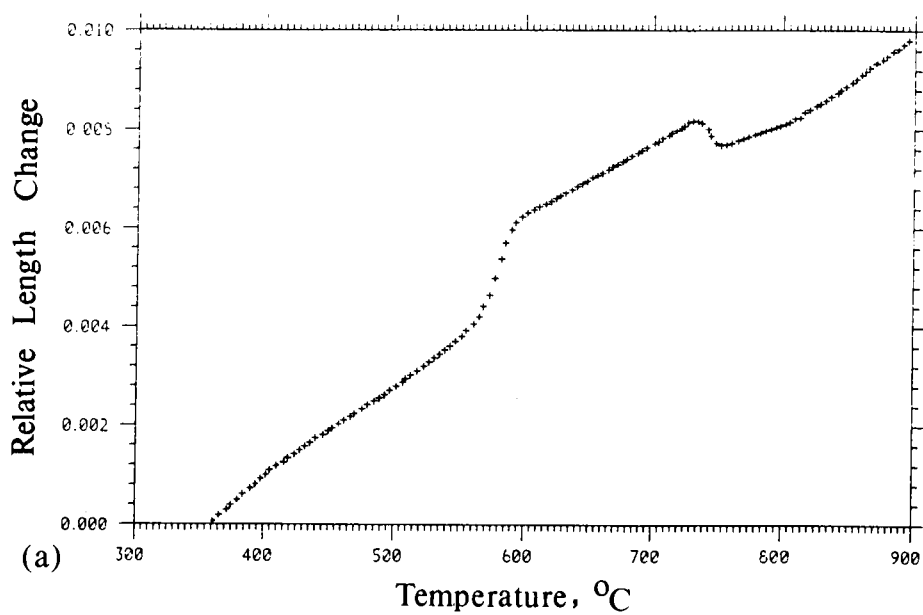
Temperature, ^{O}C

Figure VII.4(a) and (b) - Showing the relative length change versus temperature curves at heating rates, 0.06 and 0.15°C/s respectively, after isothermal transformation at 350°C for 10 minutes.

166

a

0·5 μm

b
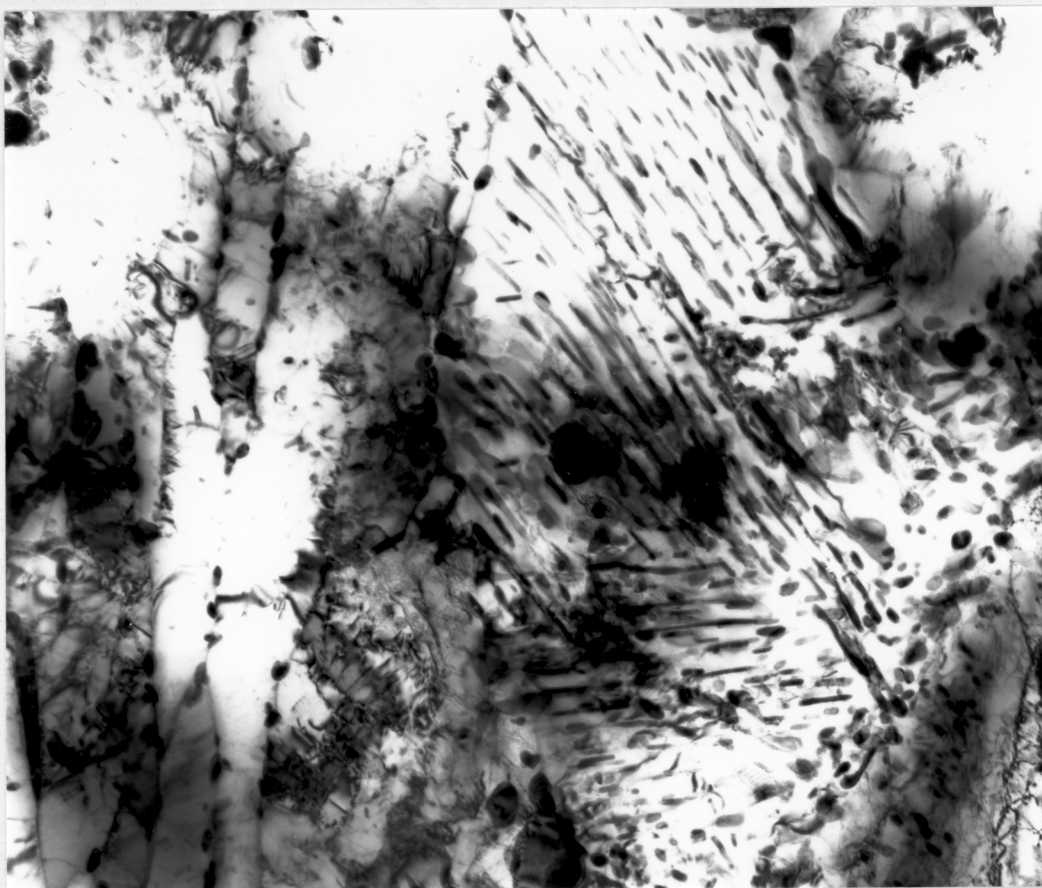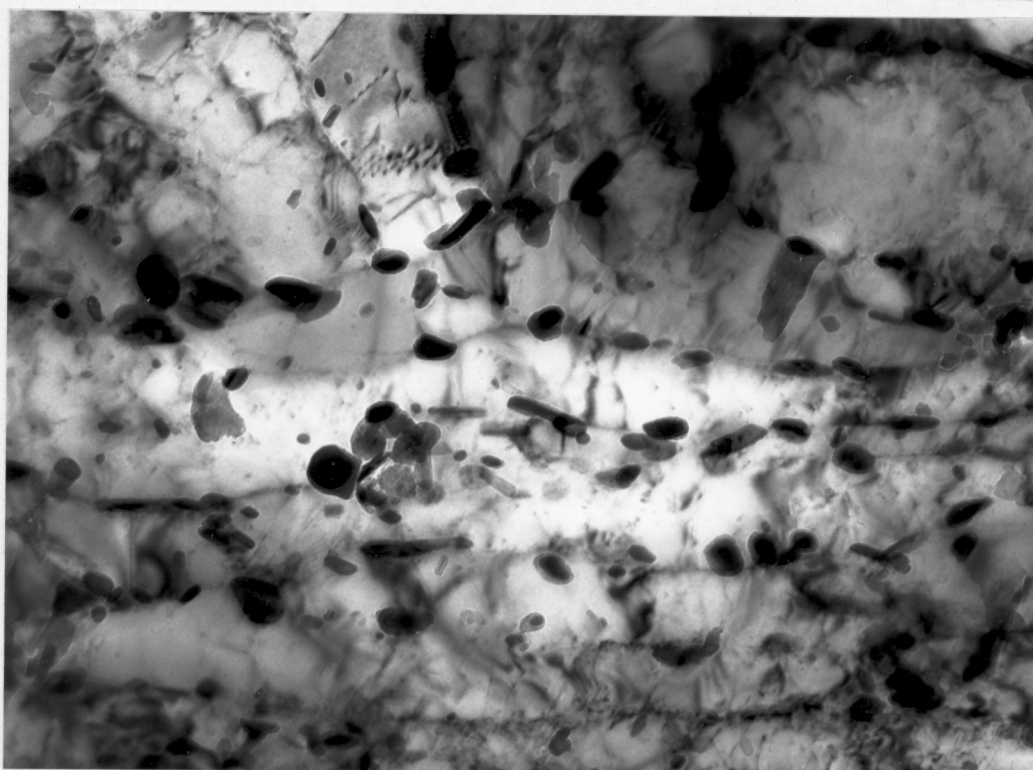
0·5 μm

Figure VII.5 - 10 mins @ 950°C → 10 mins @ 350°C → continuous heating until 600°C (heating rate = 0.06°C/s) → quenched by helium gas. (a) Electron micrograph showing a pearlite-like microstructure. (b) Electron micrograph showing the discretely nucleated carbides.

(a)

(b)
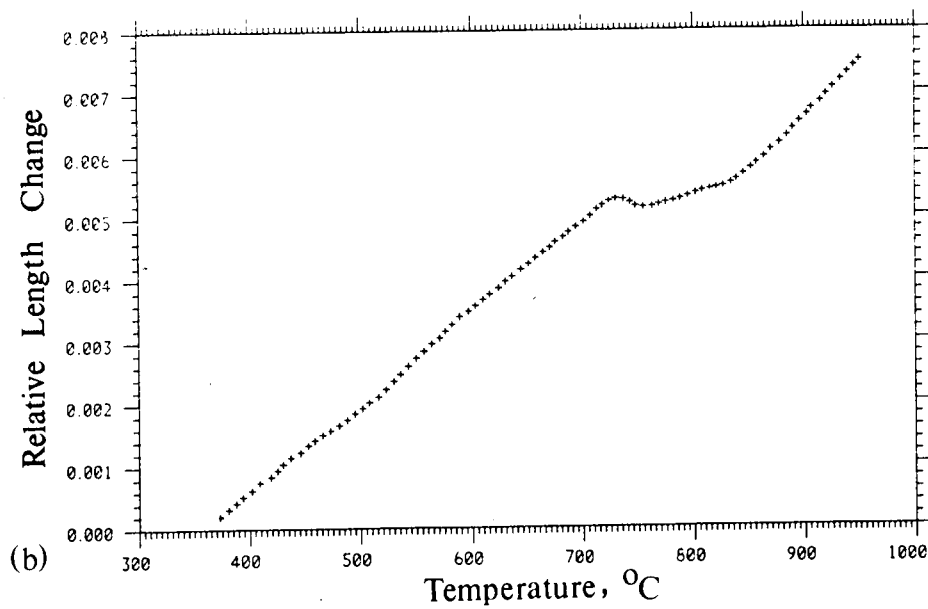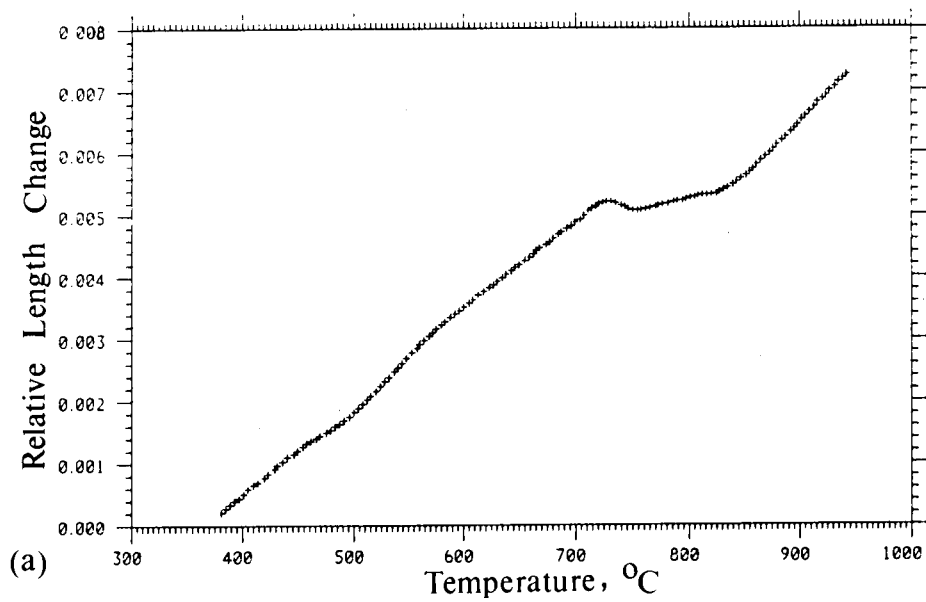
Figure VII.6(a) and (b) - Showing the relative length change versus temperature curves at heating rates 0.06 and 0.15°C/s respectively, after isothermal transformation at 350°C for 120 minutes.

168

0·5 μm
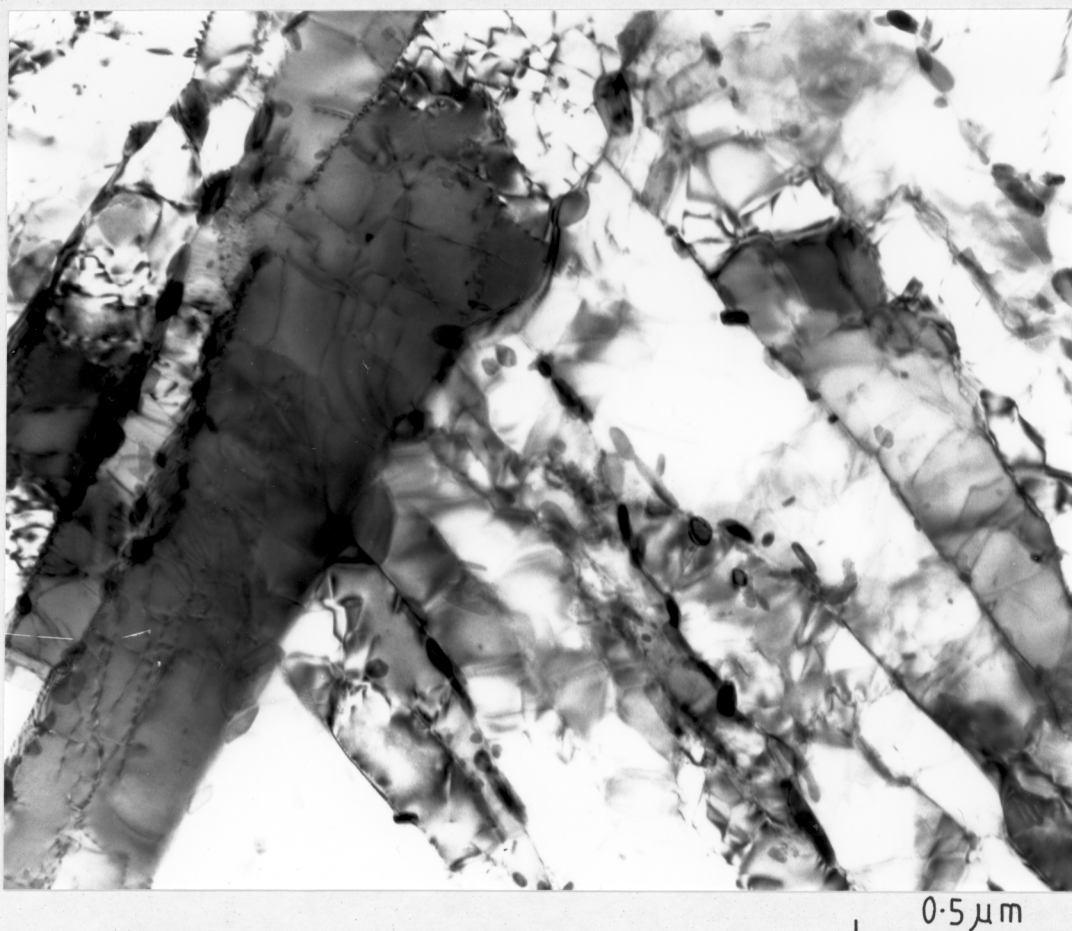
Figure VII.7 - 10 mins @ 950°C → 2 hrs @ 350°C → continuous heating until 600°C
(heating rate = 0.06°C/s) → quenched by helium gas.

0·5μm
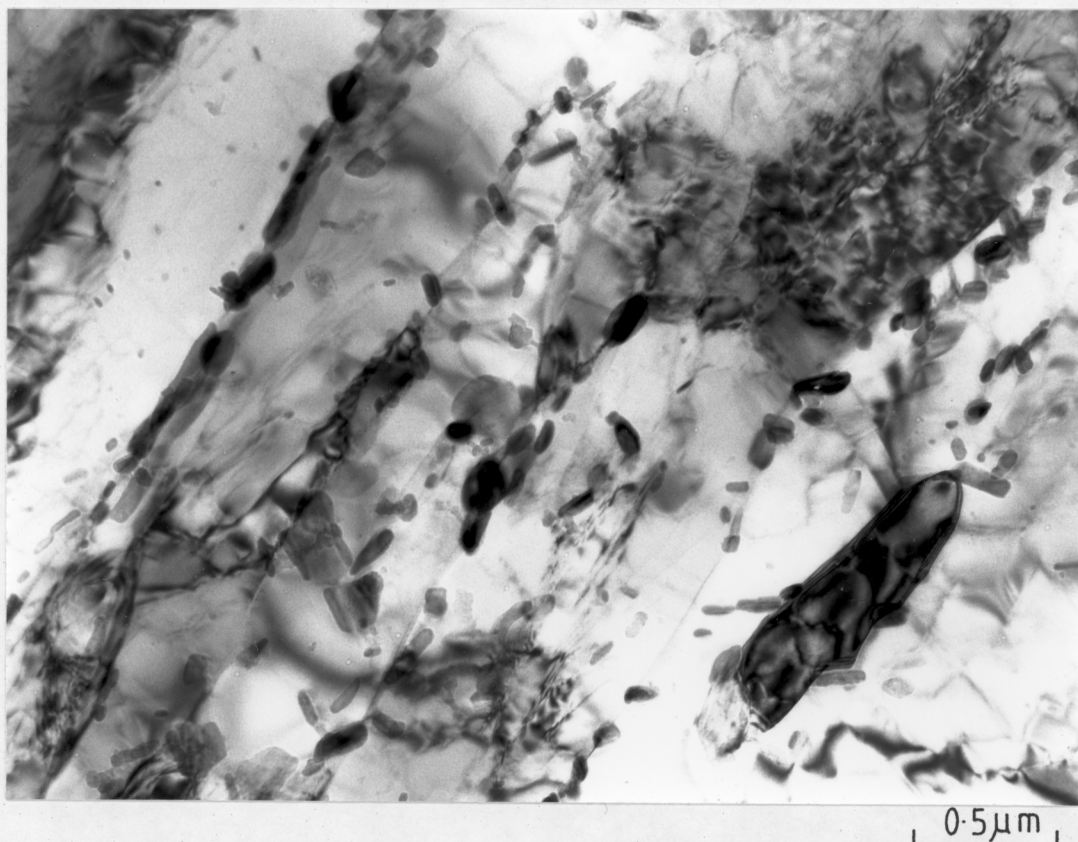
Figure VII.8 - 10 mins @ 950°C → 2 hrs @ 350°C → continuous heating until 700°C
(heating rate = 0.06°C/s) → quenched by helium gas.
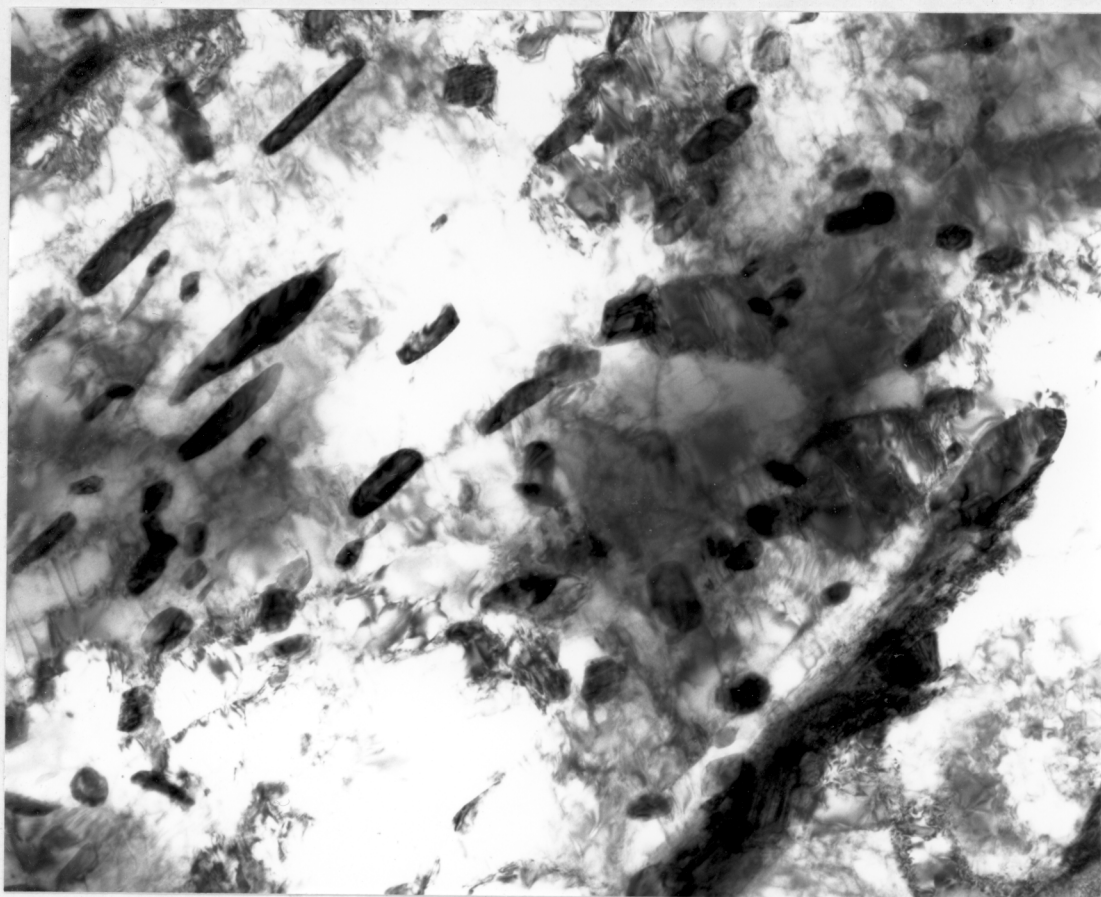
Figure VII.9 - 10 mins @ 950°C → 2 hrs @ 350°C → continuous heating until 730°C (heating rate = 0.06°C/s) → quenched by helium gas.
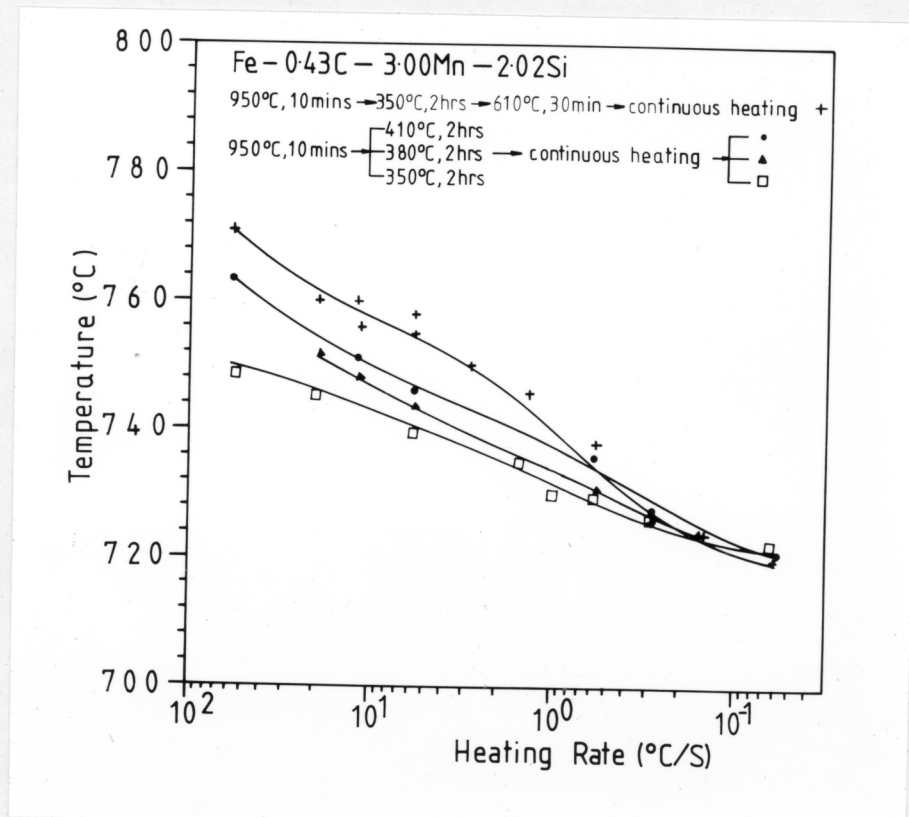
Figure VII.10 - Showing reaustenitisation start temperature versus heating rate for four different starting microstructures.
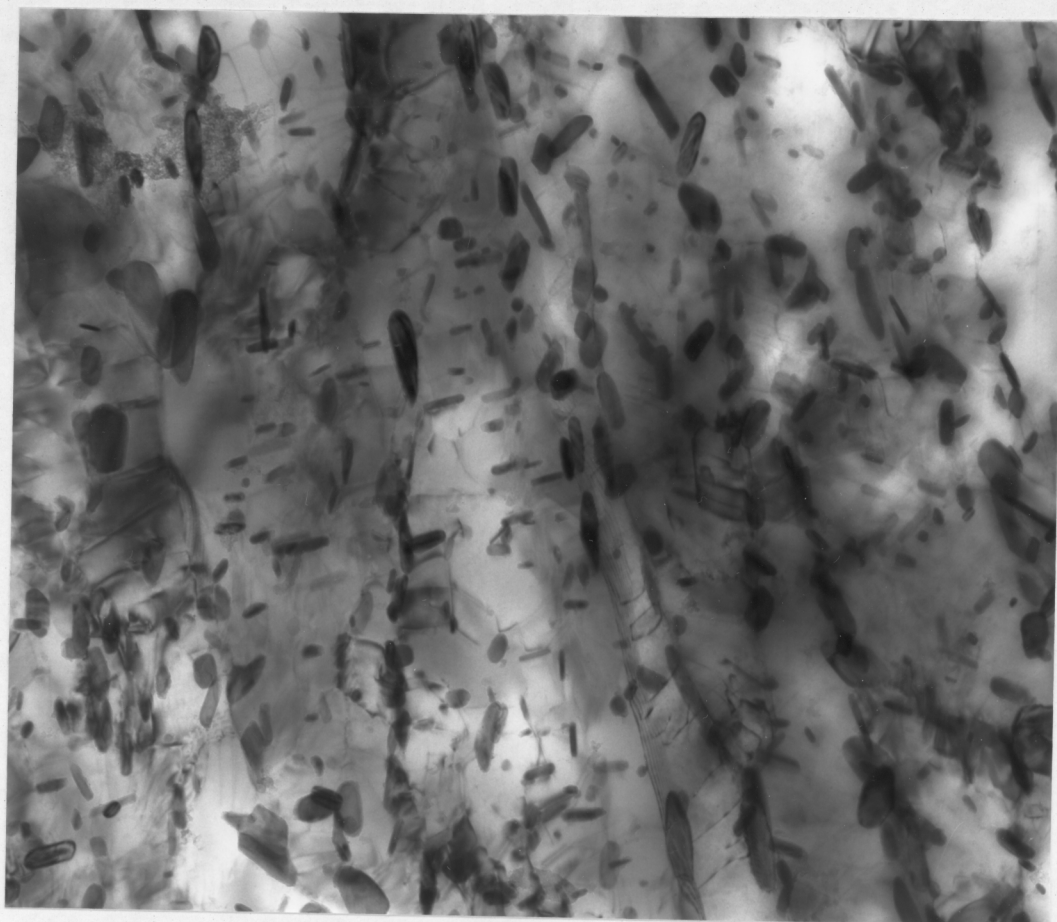
Figure VII.11 - Microstructure of tempered bainite formed by isothermal transformation at 350°C for 2 hrs, and subsequently tempered at 610°C for 30 minutes.
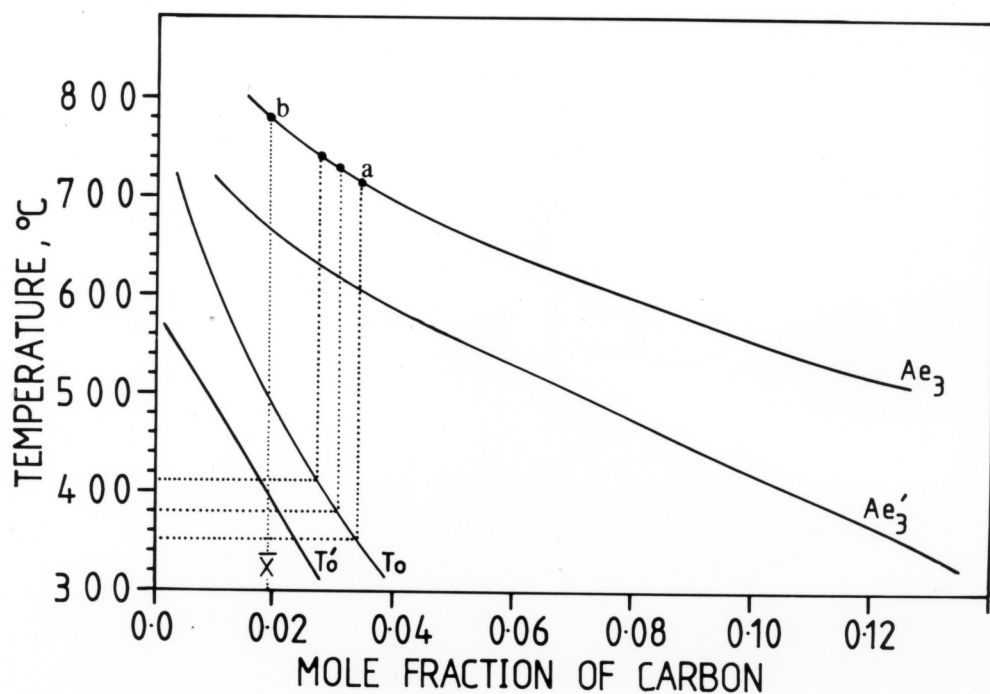
Figure VII.12 - Phase diagram showing the Ae_3, Ae_3', T_0 and T_0' for Fe-0.43C-3.00Mn-2.02Si, wt.% alloy. The Ae_3', T_0 and T_0' curves are calculated as in Ref. 89,100, and the Ae_3 curve is calculated as in Ref. 181. ($\bar{x}$ is the average carbon content of the alloy).

171
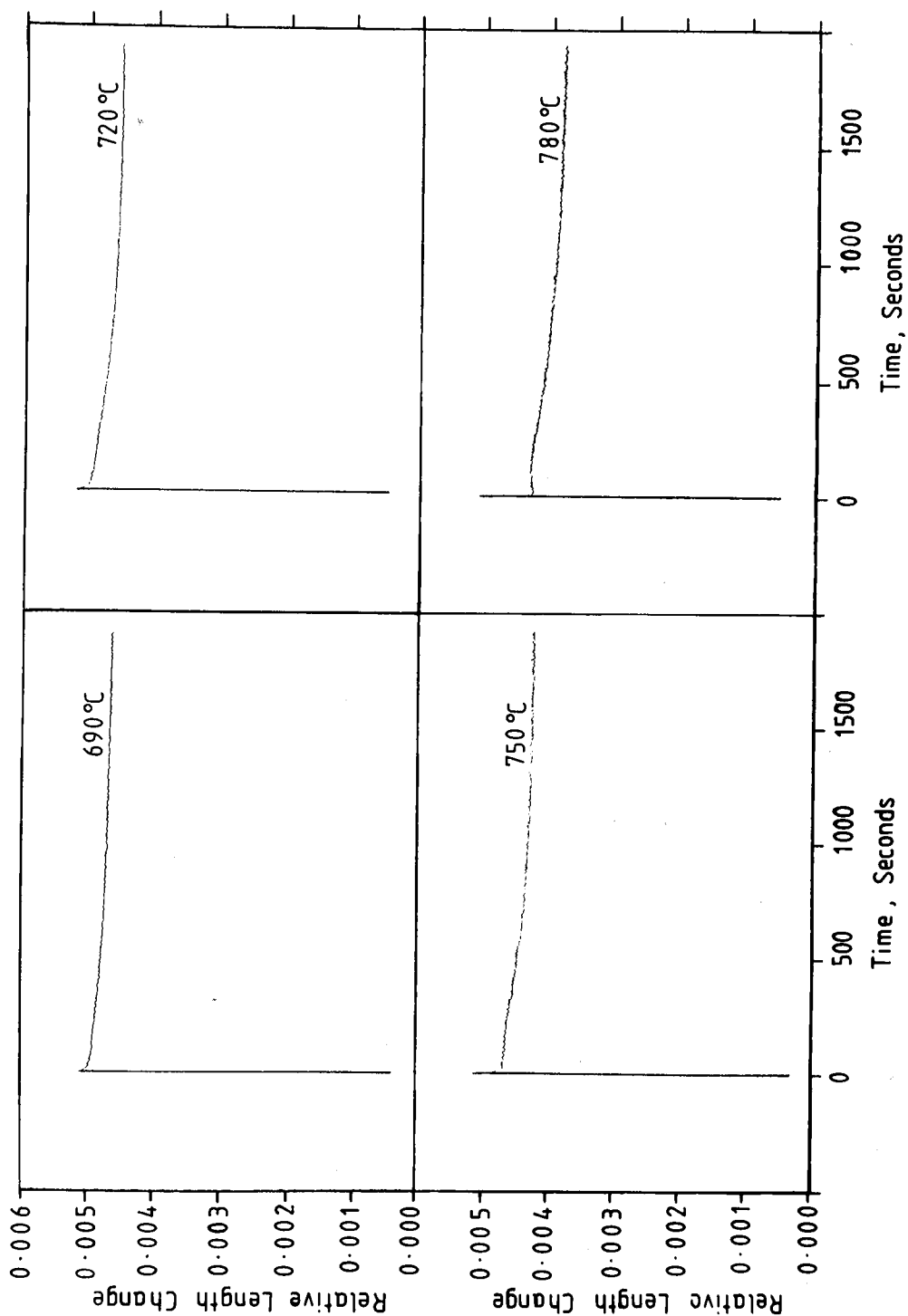
Figure VII.13 - Dilatometric curves showing isothermal reaustenitisation.

172

$0.5\,\mu m$
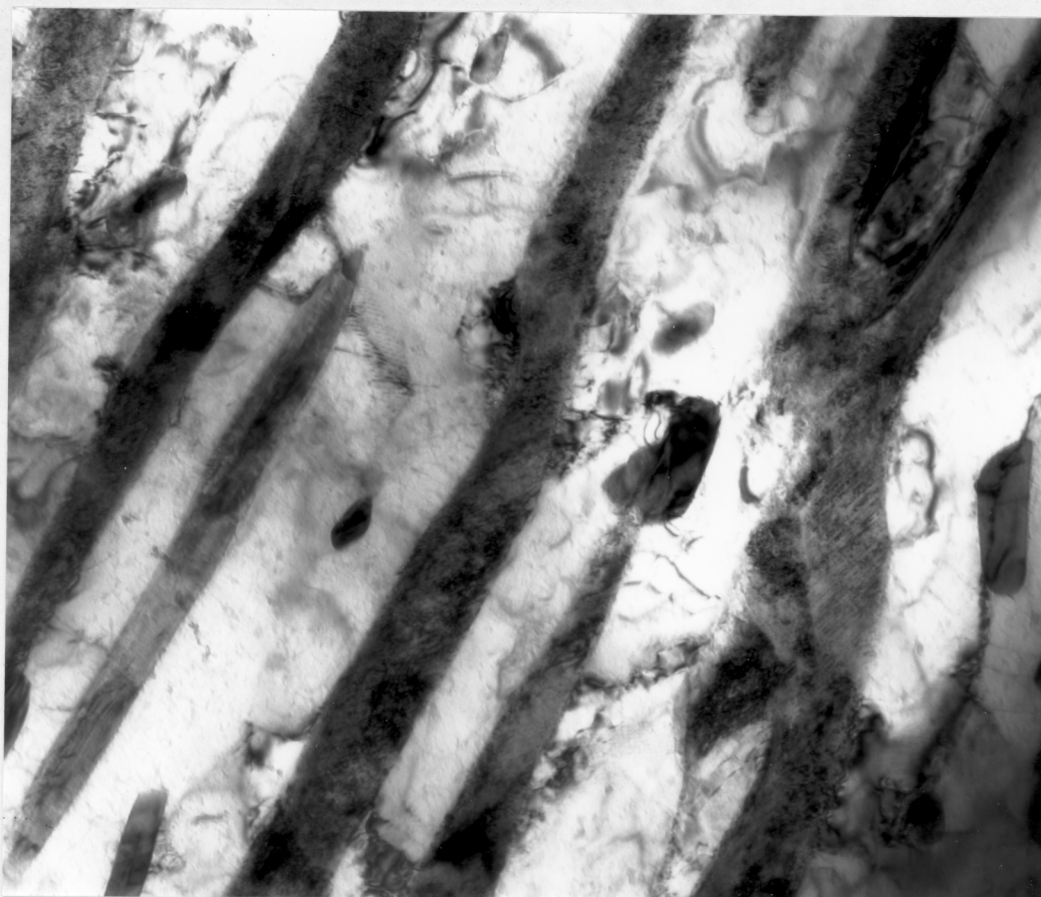
Figure VII.14a - Electron micrograph showing decomposition of austenite into carbide.
(10 mins @ 950°C → 2 hrs @ 350°C → 2 hrs @ 690°C → quenched by helium gas).
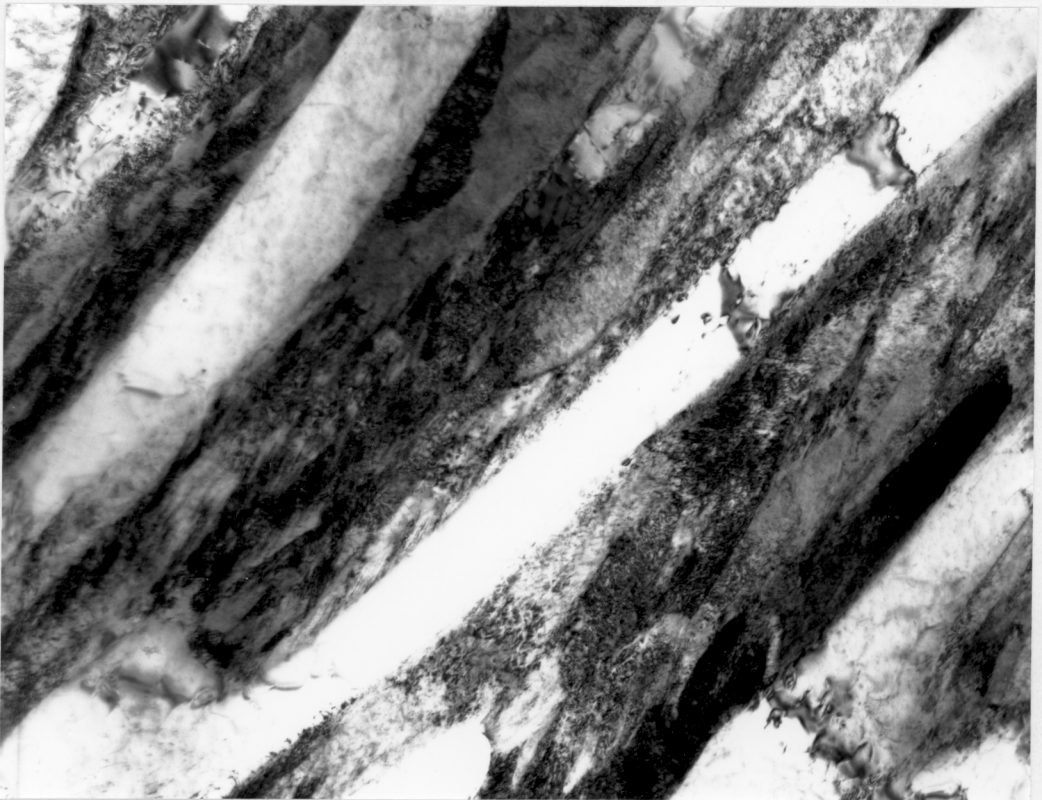

$0.5\,\mu m$
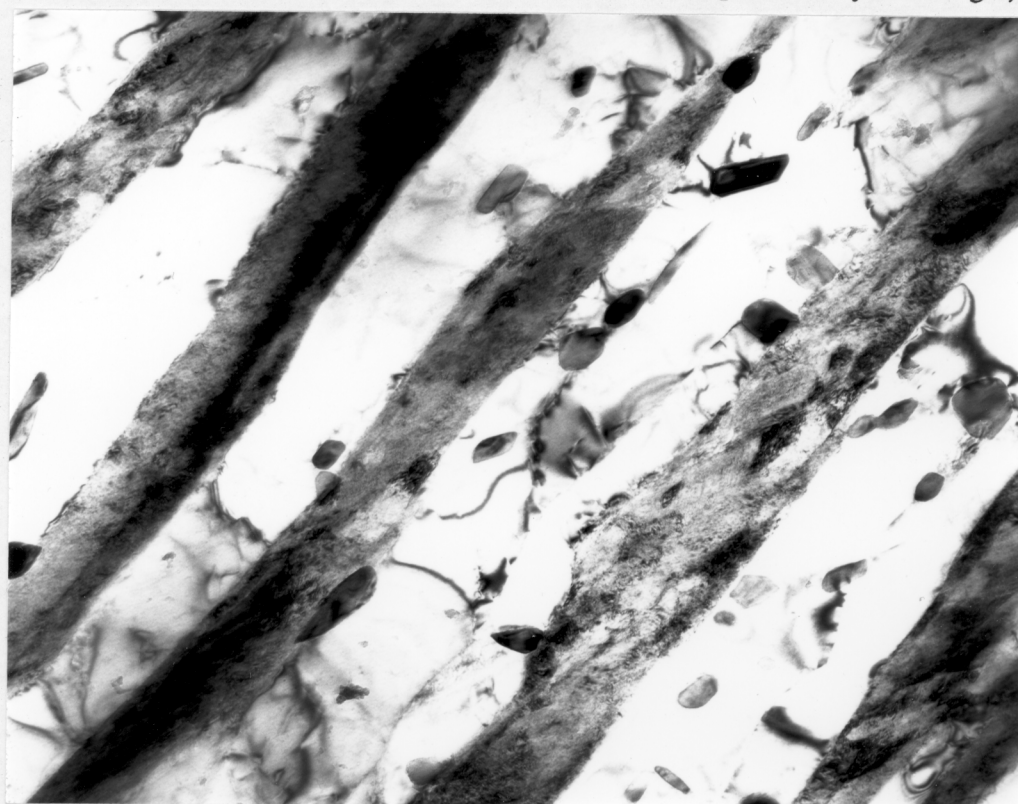
Figure VII.14b - Electron micrograph showing decomposition of austenite into carbide.
(10 mins @ 950°C → 2 hrs @ 350°C → 2 hrs @ 710°C → quenched by helium gas).
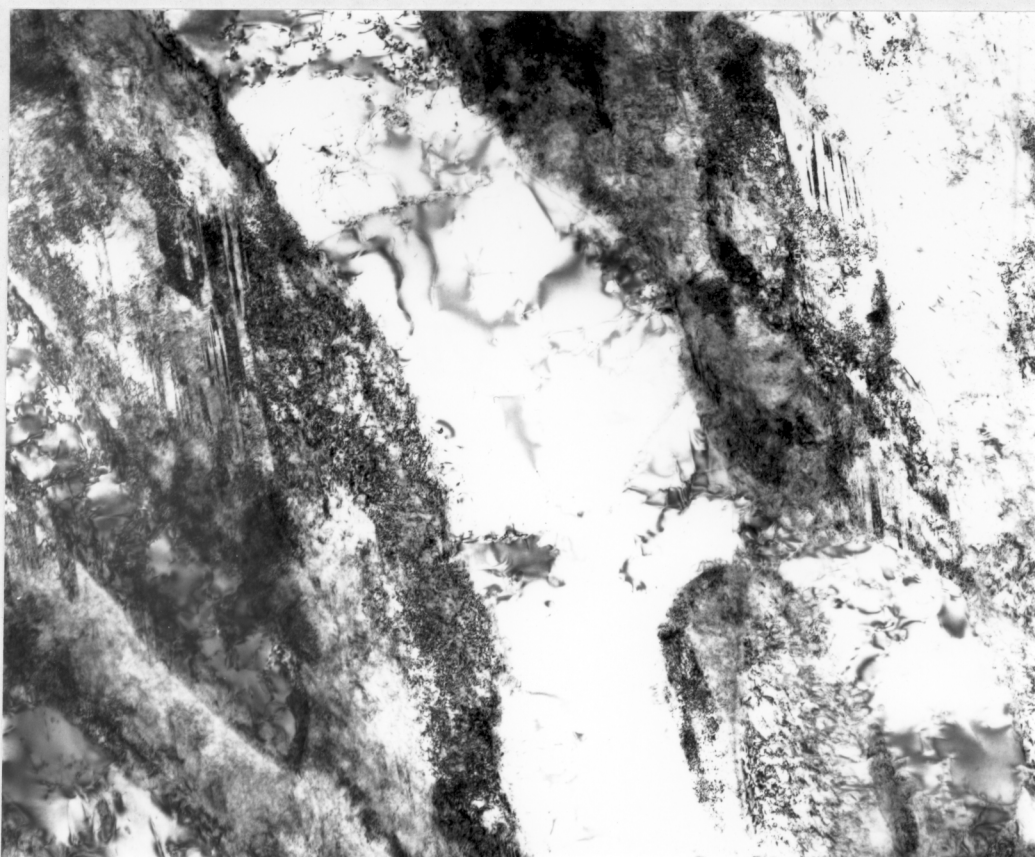
173

0·5 μm

Figure VII.14c - 10 mins @ 950°C → 2 hrs @ 350°C → 2 hrs @ 720°C → quenched by helium gas.

0·5μm

Figure VII.14d - 10 mins @ 950°C → 2 hrs @ 350°C → 2 hrs @ 750°C → quenched by helium gas.

0·5μm

Figure VII.14e - 10 mins @ 950°C → 2 hrs @ 350°C → 2 hrs @ 780°C → quenched by helium gas.

0·5μm

Figure VII.14f - 10 mins @ 950°C → 2 hrs @ 350°C → 2 hrs @ 800°c → quenched by helium gas.

175

20μm

Figure VII.14g - Optical micrograph showing the microstructure after isothermal reaustenitisation at 820°C for 2 hrs. (10 mins @ 950°C → 2 hrs @ 350°C → 2 hrs @ 820°C → quenched by helium gas).
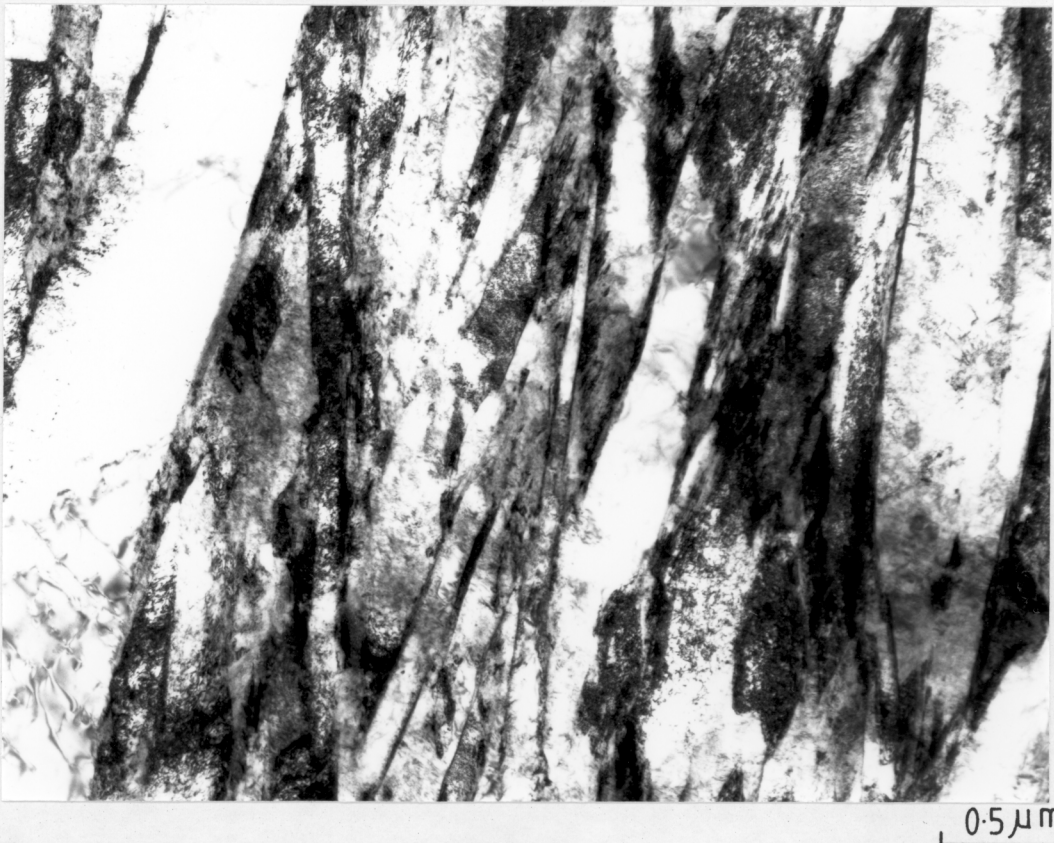

0·5μm

Figure VII.14h - Electron micrograph showing the microstructure after isothermal reaustenitisation at 820°C for 2 hrs. (10 mins @ 950°C → 2 hrs @ 350°C → 2 hrs @ 820°C → quenched by helium gas).

176

Figure VII.14i - Electron micrograph showing the microstructure after isothermal reaustenitisation at 835°C for 6.5 hrs. (10 mins @ 950°C → 2 hrs @ 350°C → 6.5 hrs @ 835°C → quenched by helium gas). A little amount of ferrite can still be found.
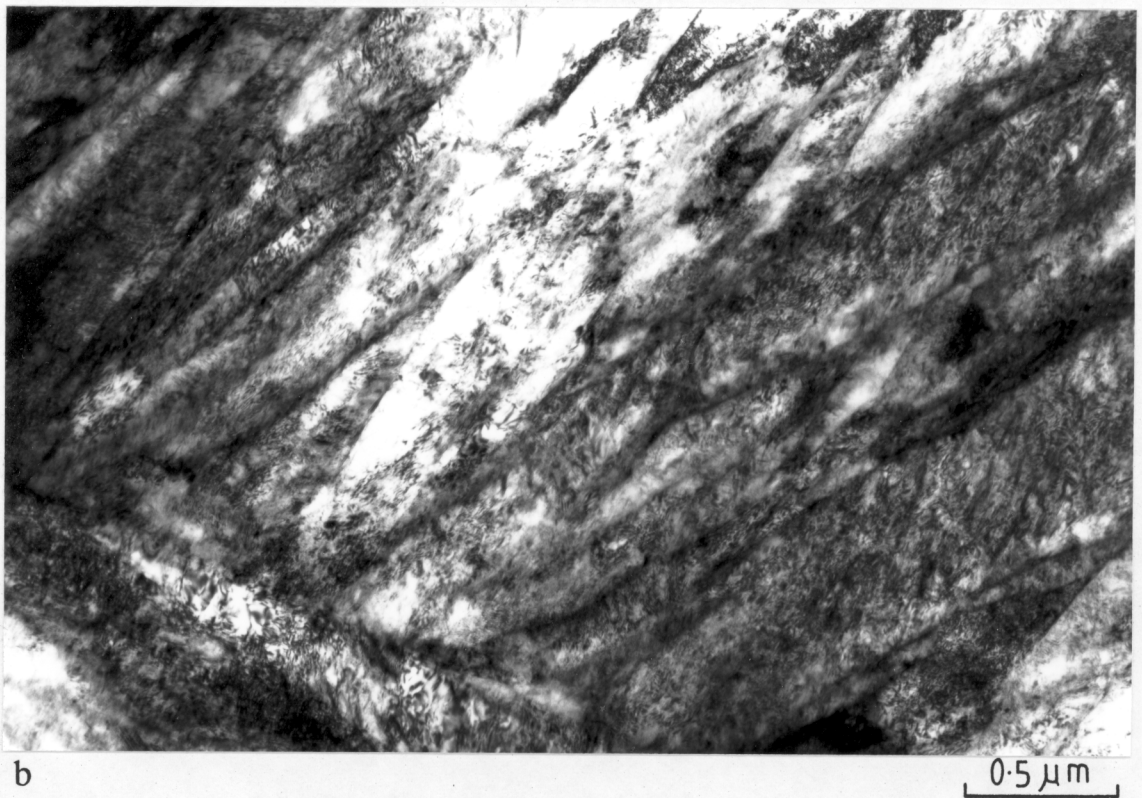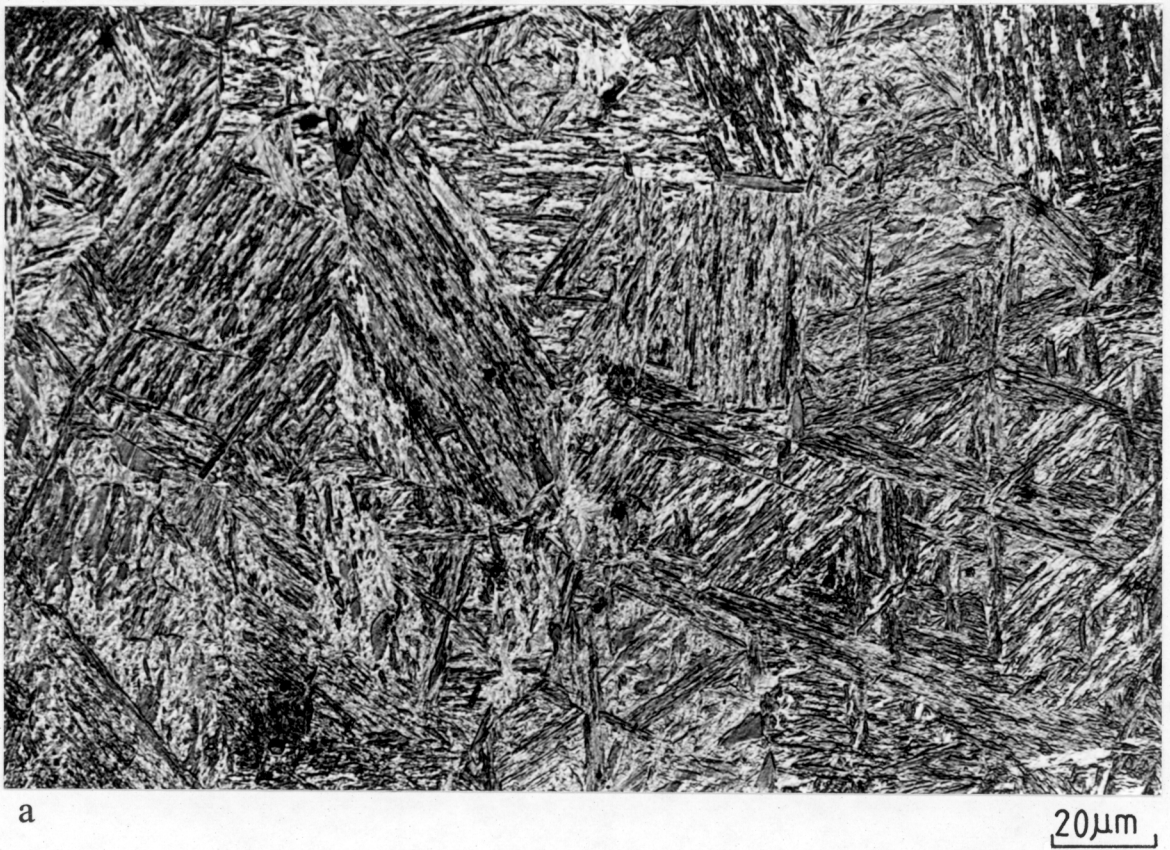
a

20μm

b

0·5 μm

Figure VII.15 - Optical micrograph (a) and electron micrograph (b) show the full martensite structure. (10 mins @ 950°C → 2 hrs @ 350°C → 168 hrs @ 780°C → water quench).
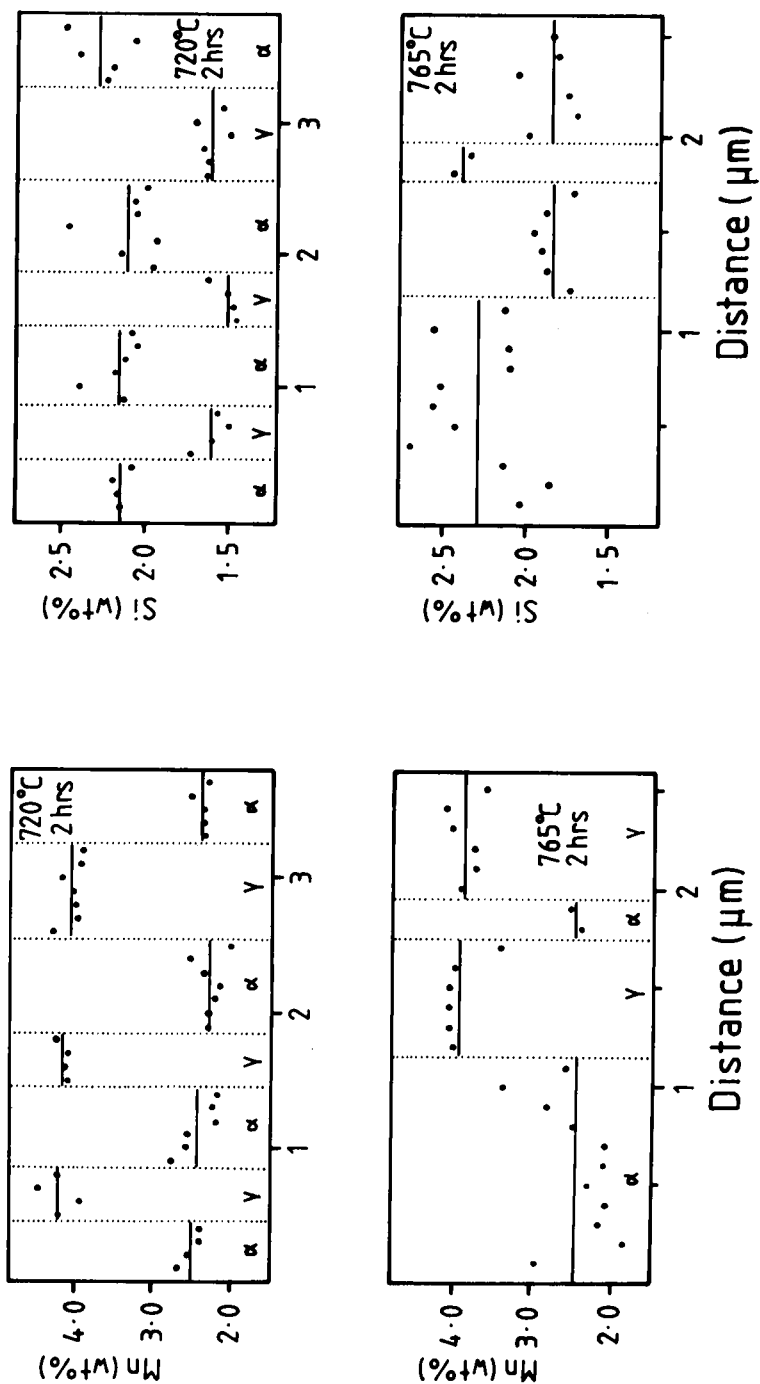
178

Figure VII.16(a) - Microanalytical data obtained using energy dispersive X-ray analysis on a Philips EM400T for specimens reaustenitised.
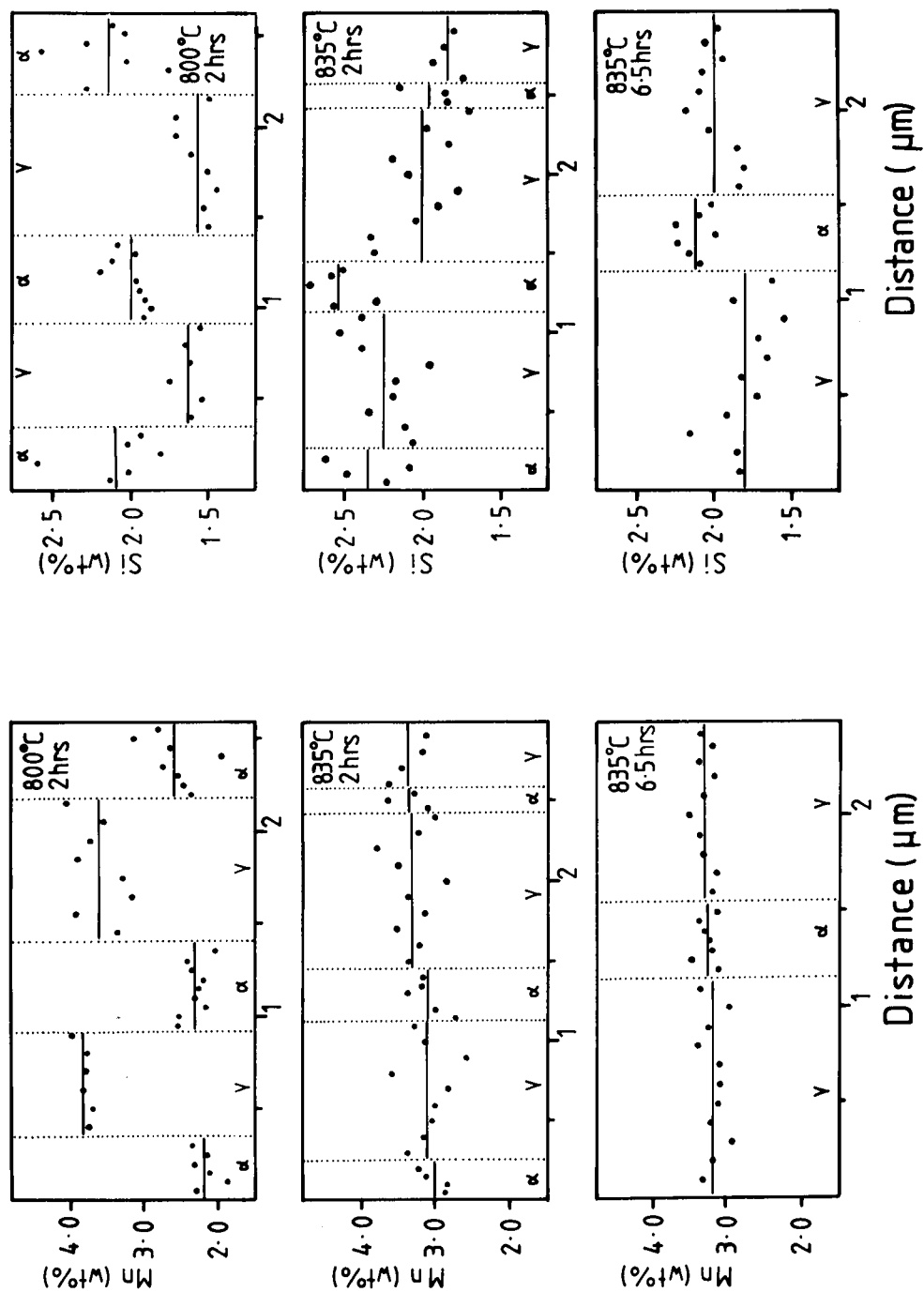
Figure VII.16(b) - Microanalytical data obtained using energy dispersive X-ray analysis on a Philips EM400T for specimens reaustenitised.